Aberrant Cortical Integration in First-Episode Psychosis During Natural Audiovisual Processing

Mäntylä, Teemu; Nummenmaa, Lauri; Rikandi, Eva; Lindgren, Maija; Kieseppä, Tuula ...

2018-11-01
Elsevier Inc.
http://hdl.handle.net/10138/301419
Mäntylä, T, Nummenmaa, L, Rikandi, E, Lindgren, M, Kieseppä, T, Hari, R, Suvisaari, J & Raij, T T 2018, 'Aberrant Cortical Integration in First-Episode Psychosis During Natural Audiovisual Processing', Biological Psychiatry, vol. 84, no. 9, pp. 655-664. https://doi.org/10.1016/j.biopsych.2018.04.014

Archival Report

Biological Psychiatry

Aberrant Cortical Integration in First-Episode Psychosis During Natural Audiovisual Processing

Teemu Mäntylä, Lauri Nummenmaa, Eva Rikandi, Maija Lindgren, Tuula Kieseppä, Riitta Hari, Jaana Suvisaari, and Tuukka T. Raij

ABSTRACT

BACKGROUND: Functional magnetic resonance imaging studies of psychotic disorders have reported both hypoactivity and hyperactivity in numerous brain regions. In line with the dysconnection hypothesis, these regions include cortical integrative hub regions. However, most earlier studies focused on a single cognitive function at a time, assessed by delivering artificial stimuli to patients with chronic psychosis. Thus, it remains unresolved whether these findings are present already in early psychosis and whether they translate to real-life–like conditions that require multisensory processing and integration.

METHODS: Scenes from the movie *Alice in Wonderland* (2010) were shown to 51 patients with first-episode psychosis (16 women) and 32 community-based control subjects (17 women) during 3T functional magnetic resonance imaging. We compared intersubject correlation, a measure of similarity of brain signal time courses in each voxel, between the groups. We also quantified the hubness as the number of connections each region has.

RESULTS: Intersubject correlation was significantly lower in patients with first-episode psychosis than in control subjects in the medial and lateral prefrontal, cingulate, precuneal, and parietotemporal regions, including the default mode network. Regional magnitude of between-group difference in intersubject correlation was associated with the hubness.

CONCLUSIONS: Our findings provide novel evidence for the dysconnection hypothesis by showing that during complex real-life–like stimulation, the most prominent functional alterations in psychotic disorders relate to integrative brain functions. Presence of such abnormalities in first-episode psychosis rules out long-term effects of illness or medication. These methods can be used in further studies to map widespread hub alterations in a single functional magnetic resonance imaging session and link them to potential downstream and upstream pathways.

Keywords: Default mode network, Disintegration, First-episode psychosis, Functional magnetic resonance imaging, Intersubject correlation, Natural stimulation

https://doi.org/10.1016/j.biopsych.2018.04.014

Schizophrenia and other psychotic disorders have been suggested to result from a compromised integration of neural signals from specialized subsystems in the brain, such as perception, language, memory, and emotions (1–3). In task-related functional magnetic resonance imaging (fMRI) studies, differences between patients with schizophrenia and healthy control subjects vary depending on the experimental task (4), with remarkably little regional overlap across tasks (5). A recent meta-analysis suggested, however, that functional changes in patients with chronic schizophrenia converge on several hub regions, such as the medial and lateral prefrontal cortex, anterior cingulate cortex, thalamus, and lateral temporal areas (5), that integrate signals from many parts of the brain (6,7). Whether such involvement of cortical hub regions occurs already in early psychosis or is simply a consequence of the chronic disorder remains unknown.

There is also no consensus regarding the most pronounced aberrations in brain function that alter the processing of the rich and complex everyday situations in patients with psychosis. Studying brain activity of subjects who view a movie provides an excellent assay for investigating such complex processing (8). An audiovisual movie can include sensory, motor, emotional, motivational, social, and cognitive contents in a narrative context. To construct a subjective understanding of the movie, the movie events must be integrated with the individual's semantic and autobiographical memory and with the present context (9,10).

Compared with resting-state fMRI studies (11), where brain activity is recorded without any specific tasks or external stimuli, fMRI recordings during a movie provide the advantage that a significant proportion of the measured brain signals reflects stimulus-driven activity that can be compared between groups and time points. In intersubject correlation (ISC) analysis (12), voxelwise functional time series is correlated with the time series of the same voxel in other individuals, providing a measure of how synchronous the brain activity of an individual is with respect to other subjects of the group.

SEE COMMENTARY ON PAGE e65

ISSN: 0006-3223

This measure has been used to study patient groups (13–17). For example, in a recent study, ISC was lower during movie viewing in patients with depression compared with a control group in regions important in the regulation of emotions and attention (17). In another study, participants with a diagnosis of Asperger's syndrome showed lower ISC in regions contributing to social information processing (15). Despite ISC analysis showing promise to reveal diagnostically relevant brain substrates of psychiatric disorders, to our knowledge, only one ISC study with 15 patients with first-episode psychosis (FEP) using naturalistic stimuli has been conducted (18).

Disintegration is a central tenet in theories of psychotic disorders (19). In terms of graph theory, measures of centrality estimate how connected a certain region of the brain is to other regions (20). In this approach, highly connected regions are often coined as hubs (21). Hubs are involved in higher-order, multisensory processing (21,22), presumably integrating information from areas with which they are connected (21,23,24). Thus, as a measure of hubness and integration of brain areas, we calculated the regional weighted degree centrality across the brain.

In the current study, we used ISC analysis to compare brain activations during a movie presentation between patients with FEP and control subjects. As the boundaries between reality and fantasy are distorted in patients with psychotic disorders, the stimulus involved scenes from the movie *Alice in Wonderland* (2010) containing both realistic and fantasy material. We expected ISC to be lower in patients with FEP, especially in brain regions relevant for multimodal, higher-level processing and integration—as determined by the region's hubness—such as the medial parietal and frontal and lateral prefrontal regions. Furthermore, we hypothesized such regions to be associated, at least in part, with the fantasy content of the movie.

METHODS AND MATERIALS

This study is a part of the Helsinki Early Psychosis Study from which we have recently published a machine-learning study (25) that focused on transient moment-to-moment changes of fMRI signals during movie viewing. Although we used almost identical data here, the research question and analysis methods were different, as we now focused on ISC between signal time courses during the entire 7-minute, 20-second movie stimulus.

Participants

The Ethics Committee of the Hospital District of Helsinki and Uusimaa approved the study (diary numbers 257/12/03/03/2009 and 226/13/03/03/2013), and all participants gave written informed consent before participation. Capacity of patients to give informed consent was assessed by the clinician responsible for treatment. From hospitals and outpatient clinics of the Helsinki University Hospital and the Department of Psychiatry, Helsinki City Health Department, we recruited 51 patients with FEP (18–40 years of age) who were having their first contact with psychiatric care for a psychotic disorder. Psychotic symptoms were evaluated with the Brief Psychiatric Rating Scale–Extended (26). The inclusion criterion was scoring $\geq$4 in the items either for Unusual Thought Content or for Hallucinations. Patients with substance-induced psychotic disorder or psychotic disorder owing to a general medical condition were excluded. Diagnostic assessment was done on the basis of the Research Version of the Structured Clinical Interview for DSM-IV Axis I Disorders interview (27) and on a careful review of all medical records by a senior psychiatrist (JS). Current medication use was asked in the interview and confirmed from medical records. The clinical assessment of the patients and control subjects has been previously described in more detail (28).

We recruited 32 control subjects of the same age group through the Finnish Population Register Centre, excluding subjects who were not eligible for MRI; had a history of psychosis; or had a chronic neurological, endocrinological, or cardiovascular disease. Patients with FEP who had epilepsy or structural brain anomalies or who were not eligible for MRI were excluded from this analysis. All participants had normal or corrected-to-normal vision.

Acquisition of fMRI Data

Owing to a scanner update during the study, we acquired fMRI data with two 3T MRI scanners at Aalto AMI Centre, Aalto NeuroImaging, Aalto University School of Science: first with a Signa VH/i scanner (GE Healthcare Ltd., Chalfont St Giles, United Kingdom) with a 16-channel head coil and later with a MAGNETOM Skyra scanner (Siemens Healthcare, Erlangen, Germany) with a 32-channel coil. The imaging parameters were the same for both scanners. Whole-brain blood oxygen level–dependent (BOLD) signal data were acquired with a gradient echo-planar sequence (repetition time 1.8 seconds, echo time 30 ms, flip angle 75°, field of view 24 cm, matrix size 64 $\times$ 64, 36 slices with a thickness of 4 mm). Fourteen patients and 11 control subjects were studied with the Signa VH/i scanner, and 37 patients and 21 control subjects were studied with the MAGNETOM Skyra scanner. We included participants from both scanners in the same analysis because multisite fMRI studies have shown that a 10% increase in total sample size will increase statistical power as opposed to using only single-scanner data (29). T1-weighted structural images with 1-mm^3 isotropic voxels and T2-weighted structural images were also acquired, and a clinical neuroradiologist evaluated these scans for brain abnormalities.

Movie Stimulus

During fMRI, the participants were shown five episodes in sequence from the movie *Alice in Wonderland*, directed by Tim Burton (Walt Disney Pictures, Burbank, CA, 2010; dubbed in Finnish) (total duration 7 minutes, 20 seconds equaling 245 echo-planar imaging volumes). This film is in part animated, but human actors are present in every scene. The scenes show Alice's wedding followed by her trip through a rabbit hole to Wonderland and subsequent fantasy events [see (25) for detailed description]. The movie was projected onto a semi-transparent screen centered in the participant's visual field, and stimulus timing was controlled by Presentation Software (Neurobehavioral Systems, Inc., Berkeley, CA). Sound was conveyed through plastic tubes, which were attached to porous ER3-14A (Etymotic Research Inc., Elk Grove Village, IL) earplugs. To insulate scanner noise, foam pads were placed inside and outside the head coil. The volume of the audio track was adapted according to the participant's subjective

preference, ensuring it was loud enough to be clearly audible over scanner noise.

Analysis of ISC Images

Computation of Voxelwise ISC. Functional volumes were preprocessed in FSL (http://www.fmrib.ox.ac.uk/fsl/). They were first realigned for movement correction, coregistered with the structural images, normalized to Montreal Neurological Institute template, and smoothed with a Gaussian kernel with 8-mm full width at half maximum. After regressing out individual head motion, we used ISC toolbox (30) to compute the voxelwise temporal Pearson correlation between every pair of subjects. To allow between-group comparisons, ISCs were calculated separately for the patient and control groups. This resulted in subjectwise ISC images, where voxel intensities reflect how similar each voxel's time course was in relation to the other subjects in the same group. A similar approach has been used in recent between-group ISC comparisons in Asperger's syndrome (15) and depression (17). We calculated the ISCs separately for participants studied with different scanners. Before the ISC images were entered into group-level analyses, they were smoothed with an 8-mm full width at half maximum kernel to account for inaccuracies in normalization and to enhance comparability between groups and scanners.

Group-Level Analysis. ISC differences between the groups were analyzed using nonparametric two-sample tests with SPM (http://www.fil.ion.ucl.ac.uk/spm/) extension SnPM13 (http://warwick.ac.uk/snpm) and 5000 permutations. We pooled the ISC images from both scanners owing to good agreement between different scanners in previous functional imaging studies (31–33). The results of ISC analyses were thresholded at familywise error–corrected voxelwise $p < .05$ and an extent of 20 contiguous voxels. The anatomical locations of statistically significant clusters were identified with Automated Anatomical Labeling (34) as implemented in the XjView toolbox (http://www.alivelearn.net/xjview). As a further characterization of the spatial distribution of ISC differences, we calculated the overlap of the group difference map with resting-state networks of a liberally thresholded seven-network parcellation map of the cerebral cortex (35). This parcellation was chosen because of its availability and popularity as well as big sample size (1000 subjects). The results were visualized using MRIcroGL (http://www.mccauslandcenter.sc.edu/mricrogl/home).

We also extracted signal time courses from 1) the regions that were most strongly synchronized in patients and control subjects during the movie (auditory and visual areas shown in Supplemental Figure S1) and 2) the regions showing the largest group difference (default mode network [DMN]). Group differences in each time point were studied to find common features of the movie that might contribute to the results. See Supplemental Methods for details.

Rating of Movie Content by an Independent Control Group

Because the separation of reality from fantasy is considered central in psychoses, an independent group of healthy control subjects (n = 17, 10 men and 7 women, mean age 26.5 years) not participating in the fMRI recording rated the moment-to-moment realism of the movie events. Each participant was asked to evaluate, by moving a mouse on a continuous scale, how likely the currently seen events would happen in real life (see http://emotion.utu.fi/softwaredata/). The data were recorded as a value between 0 (very unlikely) and 1 (very likely) every 200 ms and were downsampled to 1 repetition time to be used in modeling brain activity. This regressor was entered into a general linear model in first-level SPM analysis. Mean optic flow (36) was added as a nuisance covariate to control for visual changes based on the movement of objects in the scene. The resulting contrast images were then compared between groups as well as analyzed as one pooled sample with SnPM to show areas where BOLD signal associated significantly with the fantasy ratings across patients and control subjects. ISC differences were then corrected for multiple comparisons within these areas to show whether brain areas related to fantasy processing and ISC differences overlap.

Control for Potential Confounders

Attentional differences might account for some group differences in ISC because attention modulates sensory and cognitive processing (37–42). To control for attentional differences across groups, we computed a map of ISCs in the auditory and visual cortices balanced for scanners and groups (11 subjects included from each group for each scanner, total n = 44). This map was thresholded at pseudo $t > 22$ [for a definition of pseudo t, see e.g. (43)] to include only those brain regions that showed the strongest ISC across participants, i.e., the visual and auditory cortices (Supplemental Figure S1). We then extracted eigenvariates for subjectwise ISCs in this mask. These eigenvariates were entered as a nuisance covariate in a whole-brain ISC group comparison. In addition, age, sex, scanner, mean framewise head movement computed according to Jenkinson *et al.* (44), and chlorpromazine daily dose equivalents calculated according to Andreasen *et al.* (45) [except for sertindole, which was not available in Andreasen *et al.* and was calculated according to Haukka *et al.* (46)] were entered as nuisance covariates to exclude potential confounds in the group ISC analyses. As a complementary control for attentional confounds, we report results in the Supplemental Results where the group differences are controlled by extracted ISCs from the dorsal attention network. To further exclude confounding factors, we studied ISC group differences separately for subgroups of patients divided by median framewise displacement and for the Siemens scanner subgroup (Supplemental Results). We also plotted ISC values to identify outliers that might contribute to findings and report a complementary ISC analysis less susceptible to outliers in Supplemental Results.

Degree Centrality and ISC Differences

To test whether the sites of ISC differences and the integrative functions of the brain coincide, we computed the Pearson correlation coefficient between the ISC group difference and hubness across voxels. We used the SPM

Table 1. Participant Characteristics

	FEP Group	Control Group	Test Statistic	*p* Value
Sex, Female	16/51 (31%)	17/32 (53%)	$\chi^2 = 3.88$	.049[a]
Age, Years	23.2 (20.9–27.8)	24.7 (23.0–33.8)	$U = 593$	.037[a]
Head Motion[b], mm	0.053 (0.037–0.076)	0.056 (0.031–0.064)	$U = 789$	.801
GAF	35 (31–40)	90 (81.3–90)	$U = 4.5$	< .001[a]
Positive Symptoms[c]	7 (3–10)	0	$U = 112$	< .001[a]
Negative Symptoms[c]	5 (3–10)	0	$U = 121$	< .001[a]
Diagnosis				
Schizophrenia	23 (45.1%)			
Schizophreniform disorder	10 (19.6%)			
Schizoaffective disorder	1 (2.0%)			
MDD with psychotic features	1 (2.0%)			
Bipolar I disorder, with psychotic features	4 (7.8%)			
Brief psychotic disorder	1 (2.0%)			
Psychotic disorder NOS	11 (21.6%)			

Values are reported as *n* (%) or median and 1st–3rd quartiles.
FEP, first-episode psychosis; GAF, Global Assessment of Functioning (74,75); MDD, major depressive disorder; NOS, not otherwise specified.
[a]Statistically significant difference.
[b]Head motion is the mean framewise displacement (see main text).
[c]Positive symptoms represent the sum score from Brief Psychiatric Rating Scale (26) items Hallucination, Unusual thought content, Bizarre behaviour, and Conceptual disorganisation. Negative symptoms represent Brief Psychiatric Rating Scale item Blunted affect and items Alogia, Anhedonia/asociality, and Avolition/apathy from the Scale for the Assessment of Negative Symptoms (76). The Brief Psychiatric Rating Scale item scores were scaled to 0–6 before calculating the sum score.

contrast image including all the brain voxels (not only voxels of significant differences) from a two-sample *t* test on ISC differences of control subjects versus patients as a group difference map. The same nuisance covariates were included as in the main analysis. Hubness was measured in control subjects as weighted degree centrality [see e.g. (47)], a measure of the amount of functional connectivity of a voxel across the brain by using the same BOLD data as in the ISC analysis. Preprocessing for the degree centrality computation included MaxCorr (25,48) to reduce movement-related artifacts, and the fMRI signals from the cerebrospinal fluid and white matter were extracted and regressed out to restrict potential confounding effects of movement. Weighted degree centrality was then computed in DPARSF (49) with a default threshold connectivity value of 0.2. SPM second-level one-sample contrast image was computed to represent mean voxelwise weighted degree among the control subjects. Voxelwise spatial correlation between the ISC difference map and the hubness map was calculated within a mask: only voxels in SPM gray matter template (threshold voxel value = 0.4) and in the map of ISC in control subjects thresholded with familywise error–corrected

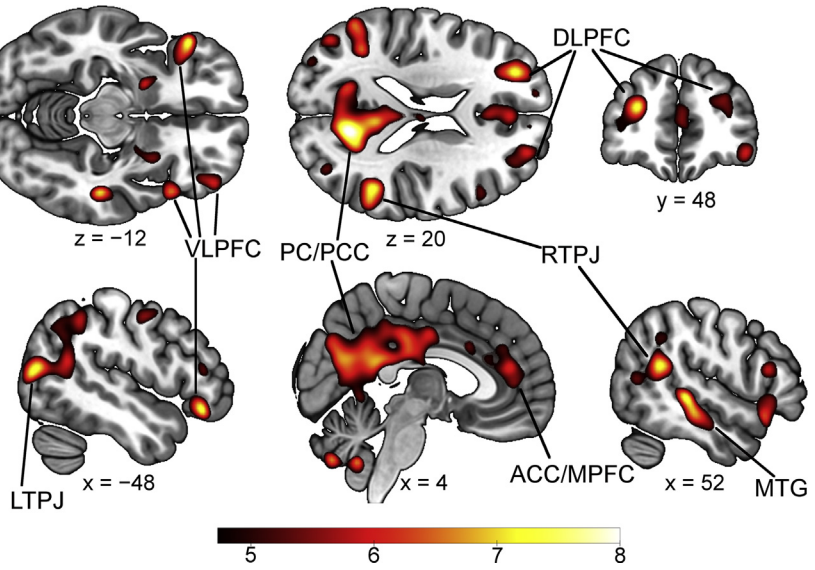

Figure 1. Differences in intersubject correlation strength, adjusted for nuisance variables (see text), between control and first-episode psychosis groups. Significantly ($p < .05$, voxel-level familywise error–corrected) stronger intersubject correlation in the control group is displayed; color bar indicates pseudo *t* value. In the transverse slices, the left hemisphere is up, and in the coronal slice, left is left. ACC/MPFC, anterior cingulate cortex/medial prefrontal cortex; DLPFC, dorsolateral prefrontal cortex; LTPJ, left temporoparietal junction; MTG, middle temporal gyrus; PC/PCC, precuneus/posterior cingulate cortex; RTPJ, right temporoparietal junction; VLPFC, ventrolateral prefrontal cortex.

voxel-level $p < .001$ were included. The ISC map was used to exclude gray matter areas with signal loss owing to susceptibility artifacts.

RESULTS

Participant Characteristics

Table 1 presents the characteristics of the participants. Patients were on average 1.5 years (median) younger than control subjects, and the patient group included more men (69% vs. 47%). Chlorpromazine equivalent daily dose was on average 365 mg (range, 0–1214 mg) in the patients.

ISC Findings

ISC was strongest in both groups in visual and auditory cortices but significantly weaker in patients than in control subjects in the bilateral precuneus/posterior cingulate cortex (precuneus/PCC), anterior cingulate cortex/medial prefrontal cortex (ACC/MPFC), posterior middle temporal gyrus (MTG), angular gyrus, supramarginal gyrus, inferior parietal lobule

Table 2. Group Comparison of Intersubject Correlations

Region	Peak (MNI) *x, y, z*	Minimum *p* Value[a]	Extent (cm^3)
Parietal, Temporal, Occipital			
Bilateral precuneus, cuneus, PCC, post MCC, and calcarine cortex	12, −64, 24	.0002	42.9
Right MTG, including STG and ITG	52, −30, −4	.0002	4.2
Left TPJ, including MOG	−48, −76, 14	.0002	13.2
Right TPJ	50, −48, 20	.0002	8.7
Left calcarine and lingual gyri	−24, −66, 4	.0004	0.7
Right post insula and Heschl's gyrus	38, −20, 12	.0046	0.7
Right fusiform gyrus	34, −38, −20	.0074	0.2
Right MOG	36, −78, 20	.0078	0.6
Left MOG	−34, −82, 28	.0012	1.9
Frontal			
Left DLPFC	−28, 46, 18	.0002	6.0
Left VLPFC, including STP	−48, 32, −12	.0002	4.5
Right ant VLPFC, including STP	48, 22, −16	.0002	2.7
Right post VLPFC	46, 22, 14	.0002	1.5
Bilateral ACC, ant MCC, and MPFC	0, 16, 32	.0004	5.4
Left pre- and postcentral gyrus	−52, −6, 48	.0010	1.0
Right DLPFC	26, 54, 20	.0010	6.9
Right orbitofrontal cortex	44, 48, −12	.0010	1.2
Left ant SFG and medial SFG	−14, 60, 24	.0010	0.4
Right SMA and medial SFG	8, 24, 60	.0034	0.6
Left post SFG and medial SFG	−10, 34, 52	.0038	0.6
Left SMA	−8, 10, 66	.0044	0.8
Right post MFG and precentral gyrus	34, −2, 52	.0078	0.6
Subcortical			
Left cerebellum (8)	−28, −62, −60	.0002	0.6
Bilateral cerebellum (9 and vermis 9)	6, −56, −46	.0002	1.4
Right cerebellum (7b, 8, and vermis 8)	4, −74, −44	.0002	0.9
Right cerebellum (8 and 10)	32, −40, −46	.0002	0.4
Left putamen	−20, 4, −10	.0010	0.6
Left cerebellum (crus 2 and 7b)	−22, −82, −44	.0012	1.1
Right cerebellum (8)	26, −62, −60	.0014	0.3
Left cerebellum (6 and crus 1)	−40, −52, −28	.0044	0.2
Right putamen	28, 8, −12	.0046	0.8
Left caudate nucleus	−12, 2, 8	.0096	0.5
Right thalamus	8, −12, 2	.0140	0.2

This table shows where intersubject correlations are higher in control subjects.

ACC, anterior cingulate cortex; ant, anterior; DLPFC, dorsolateral prefrontal cortex; ITG, inferior temporal gyrus; MCC, midcingulate cortex; MFG, middle frontal gyrus; MNI, Montreal Neurological Institute; MOG, middle occipital gyrus; MPFC, medial prefrontal cortex; MTG, middle temporal gyrus; PCC, posterior cingulate cortex; post, posterior; SFG, superior frontal gyrus; SMA, supplementary motor area; STG, superior temporal gyrus; STP, superior temporal pole; TPJ, temporoparietal junction; VLPFC, ventrolateral prefrontal cortex.

[a]Familywise error–corrected for multiple comparisons. Minimum *p* value derives from a permutation test with 5000 permutations. Extent refers to contiguous voxels below threshold *p* value.

(the latter four regions called temporoparietal junction [TPJ] for convenience), middle and inferior frontal gyrus (called dorsolateral prefrontal cortex and ventrolateral prefrontal cortex, respectively, for convenience), superior frontal gyrus, putamen, cerebellum, and occipital regions, as well as in right Heschl's gyrus/posterior insula, thalamus and MTG, and left precentral gyrus, postcentral gyrus, and caudate nucleus (Figure 1 and Table 2; see Supplemental Table S1 for mean ISC from all clusters for patients and control subjects). These differences remained statistically significant when adjusted for potential confounding effects of the ISCs from visual and auditory cortices (a proxy of attention to the stimulus) (see also Supplemental Results, Supplemental Table S2, and Supplemental Figure S4 for dorsal attention network-controlled results), age, sex, head movement, scanner, and antipsychotic dose equivalents. Compared with the resting-state atlas (35), 40% of the cortical (i.e., excluding subcortical differences) ISC difference map overlapped with the DMN, and the overlap with the other six networks was <16% for each (Figure 2). Note that in this parcellation, the somatomotor, auditory, and posterior insular cortices are included in the same network (35). Two clusters in posterior occipital lobe (cluster size [k] = 1.1 cm^3, p = .0002, peak at x = −22, y = −94, z = 6; and k = 0.7 cm^3, p = .006, peak at x = 10, y = −90, z = −12) showed significantly higher ISC in the patient group than in the control group. However, these differences reached statistical significance only after the inclusion of the ISCs from visual and auditory cortices to the model as a nuisance covariate.

We show in the Supplemental Results that findings were similar in the high-motion (n = 26) and low-motion (n = 25) subgroups (Supplemental Figures S2 and S3). Also, the use of two scanners did not have a major effect, as most of the same clusters, as in the main analysis, showed a significant difference when using only data acquired with the Siemens scanner (Supplemental Results and Supplemental Figure S5). The ISC distributions suggest that the group differences were not driven by few deviant patients (Supplemental Results and Supplemental Figures S6–S8). Neither the z-scored signals nor the squared differences from the group mean differed statistically significantly between the groups at any time point.

Association With Degree Centrality

Figure 3 presents the overlap between ISC group difference and the weighted degree centrality of the control subjects. The highest degree was found in the precuneus/PCC, ACC/dorsal MPFC, lateral occipital, parietal, and temporal regions as well as the dorsolateral prefrontal cortex, all of which overlap extensively with areas where between-group ISC differences were found. The Pearson correlation coefficient r between the ISC group difference (control > patient) and the weighted degree centrality of the control subjects was .46 (p < .001), showing that the more functionally connected a region was, the greater the difference in its ISC between the patient and control groups.

Association of BOLD Signal With Fantasy Content of the Movie

No group differences were found in a whole-brain analysis of the association between BOLD signal and fantasy content. In a pooled sample of both patients and control subjects, the fantasy content of the movie correlated with BOLD signals of the occipital, temporal, and parietal lobes as well as of the dorsolateral prefrontal cortices (Figure 4). These regions overlapped with the ISC group difference in bilateral precuneus/PCC, TPJ, precentral, and ventrolateral prefrontal

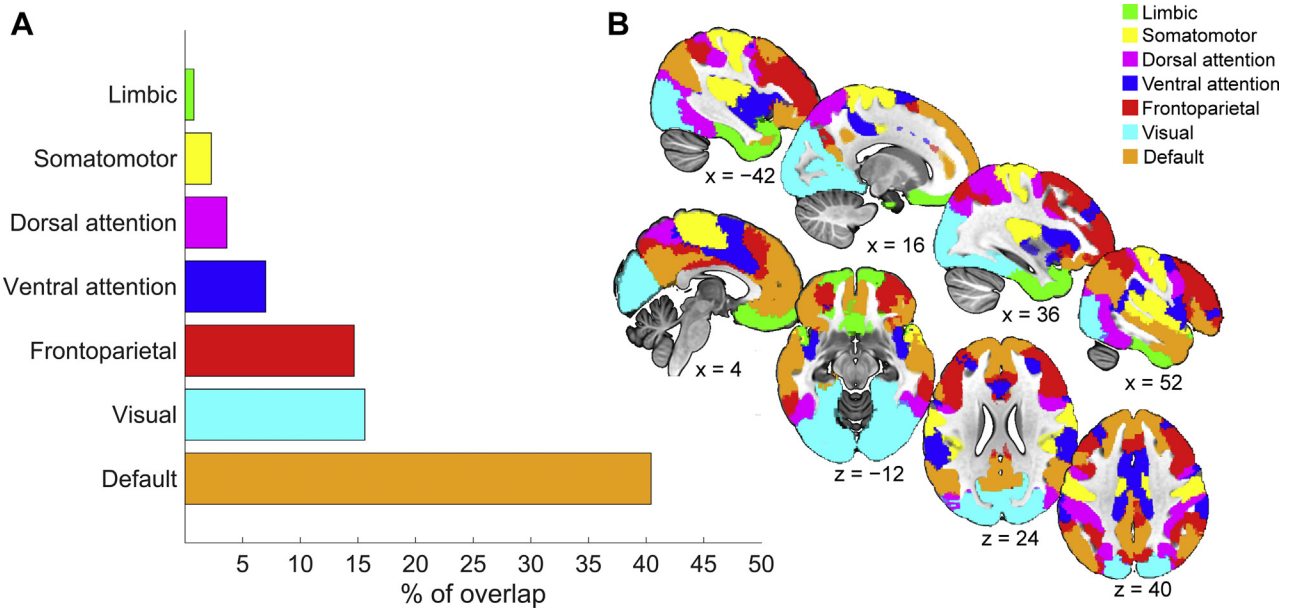

Figure 2. Overlap of the intersubject correlation difference map with different resting-state networks as described by Yeo *et al.* (35). The overlaps (shown in percentage in panel **A**) are color-coded for each network. **(B)** Selected slices from the resting-state atlas.

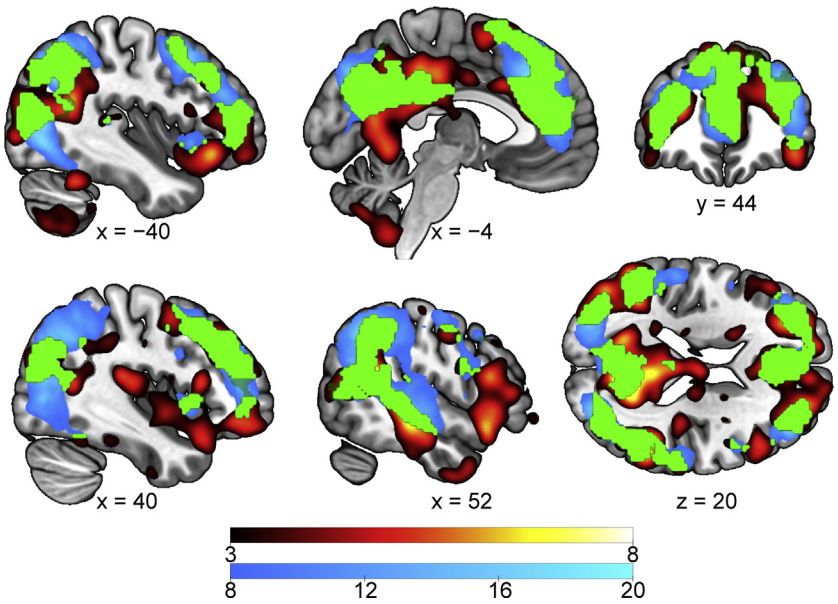

Figure 3. Overlap between degree centrality in control subjects (cool colors) and intersubject correlation difference map from the main analysis (warm colors). Overlap is shown in green. The maps are thresholded at $t > 8$ and pseudo $t > 3$, respectively, for visualization. Color bars indicate the respective statistical values. In the transverse slice, the left hemisphere is up, and in the coronal slice, left is left.

cortex and in right dorsolateral prefrontal cortex, Heschl's gyrus/posterior insula, and MTG.

DISCUSSION

We found significantly weaker ISC during movie viewing in patients with FEP than in control subjects in widespread brain regions, including bilateral precuneus/PCC, ACC/MPFC, TPJ, lateral prefrontal cortices, higher-level occipital areas, and right MTG as well as in subcortical structures. The differences between patients and control subjects remained statistically significant even after adjusting for ISCs in the visual and auditory sensory areas, which suggests that the group differences were not due to different input to primary sensory areas or due to compromised attention in the patients. Although the significant clusters in the right MTG and posterior insula/Heschl's gyrus coincided with early auditory cortical areas, the MTG cluster extended to association cortical areas and largely overlapped with lateral temporal regions of the DMN.

Mapping disorder-related brain-activity alterations that are relevant to processing of natural, dynamic, and multimodal stimuli helps in understanding how psychotic disorders contribute to everyday sensory, cognitive, and affective processing. While numerous task-selective functional brain alterations have been reported in patients with FEP, they may not directly translate to brain function during daily life (50). Natural and dynamic stimuli consistently trigger more reproducible brain activity than highly specific stimuli (51), especially in higher-level regions, and brain regions showing no net activity changes to repeated stimuli might still respond reliably to complex stimuli (52).

Several of these regions, such as the precuneus/PCC, ACC/MPFC, bilateral TPJ, and lateral prefrontal cortex (22,47), are considered as high-level areas integrating signals from multiple brain systems. Although altered low-level sensory processing

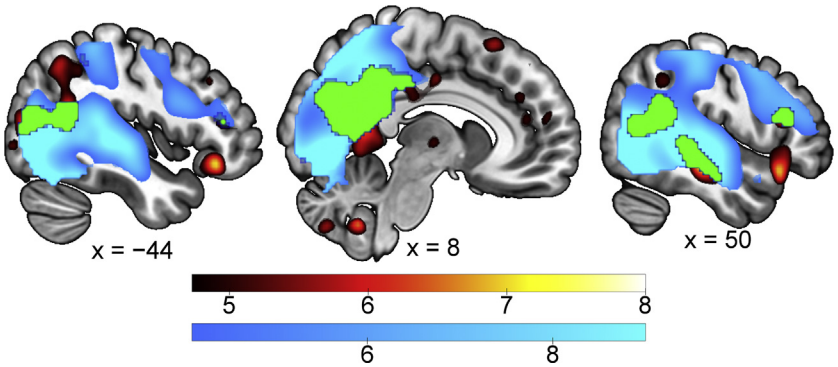

Figure 4. Association between online rating of the fantasy content of the movie and blood oxygen level–dependent signal in a pooled sample of patients and control subjects (cool colors). The intersubject correlation difference is shown (warm colors) for reference (statistical image threshold is voxel-level familywise error–corrected $p < .05$). Overlap is shown in green. Color bars indicate the respective pseudo t values.

might contribute to psychotic symptoms (53,54), the main deficits in patients with psychosis seem to result from disintegrated higher-level functions, preventing coherent, dynamic perceptions and the adaptive interaction of cognition and emotions and their appropriate contextualization through memory (2,55). The hubness, measured in control subjects, was correlated with the magnitude of ISC group differences, suggesting that the largest ISC differences predominate in hub regions. Accordingly, the current ISC differences overlapped with cortical hubs as defined in previous studies (21,22). Structural and resting-state functional imaging has shown psychosis-related alterations both in the hubs and in whole-brain network topology supporting global integration. Such alterations have been reported in patients with FEP (56), patients with chronic schizophrenia (57–59), unaffected siblings of patients with schizophrenia (60), and population-based samples of people with subclinical psychotic experiences (61). A pooled analysis on task-fMRI studies in patients with chronic schizophrenia showed overrepresentation of functional alterations in hubs compared with nonhub regions (5). Our findings imply that the prominence of hub alterations can be quantified during a single fMRI session, instead of using a set of multiple tasks (5), by employing a naturalistic movie stimulus.

Many regions where we observed ISC differences, including the bilateral precuneus/PCC, ACC/MPFC, and TPJ, overlap with the DMN (35,62–64). In our earlier machine-learning analysis using the same cohort, moment-to-moment changes in the BOLD signal differentiated patients and control subjects with an average 77.5% accuracy, based largely on the functioning of the precuneus/PCC (25). Accordingly, the statistically most significant ISC differences between the groups occurred in the central hub region of the DMN—the precuneus/PCC. DMN has been proposed to serve as a global integrator for conscious experience (65) and to be at the top end of cortical connectivity hierarchy (66). The precuneus/PCC, ACC/MPFC, and TPJ have longer temporal receptive windows than lower-level sensory areas, as evidenced by ISC analysis (67,68), and may integrate information over minutes (69). In agreement, ISC of these regions may differentiate patients with FEP and control subjects better than processing a narrative at the word or sentence level (18). In the present study, the activity in the precuneus/PCC and TPJ increased as a function of fantasy content of the movie, together with the activity of the auditory and visual cortices. Notably, the sense of reality entails comparing current sensory information with an internal model of the world based on semantic and autobiographical memory, which are related to DMN functioning (9,70).

The clustering of functional alterations to hub regions of patients with psychosis might be related to the high metabolic demands of hubs (71,72). Hub regions integrate signals from several brain networks (73) so that multiple dysfunctions across the brain could converge to them. In general, hub dysfunction might comprise a common denominator of psychotic disorders to which heterogeneous lower-level alterations contribute.

Limitations

Patients and control subjects differed in mean age and sex ratio, but controlling for these potential confounders statistically did not alter the main results. Considering the complexity of the movie stimulus, it was difficult to control for all the variables that may have contributed to the ISC findings. It could also be speculated that another kind of movie might have resulted in different findings and that some important elements for understanding the brain basis of psychosis may have been missing from the present stimulus; however, different kinds of engaging movies tend to elicit ISC in similar areas (51). Accordingly, none of the individual time points of the extracted DMN signal separated the groups in the present study.

Conclusions

The most prominent functional brain alterations in patients with FEP, observed while the patients were viewing a complex audiovisual movie stimulus, were located in hub regions that subserve integrative brain functions. The diffuse brain alterations shown in previous single-task fMRI studies on psychotic disorders might converge on the dysfunction of the integrative hubs during processing of complex real-life–like information. Present methods could be used in further studies to access both upstream and downstream pathways of hub dysfunction.

ACKNOWLEDGMENTS AND DISCLOSURES

This work was supported by the Sigrid Jusélius Foundation (JS), Finnish Cultural Foundation (TM, JS, and RH), European Research Council (Advanced Grant No. 232946 to RH), Jalmari and Rauha Ahokas Foundation (TM), Doctoral Program Brain and Mind of the University of Helsinki (TM), Academy of Finland (MIND program Grant No. 265917 to LN and Grant Nos. 278171 to JS and 251155 to TTR), Finnish Medical Foundation (TTR), Louis-Jeantet Foundation (research award to RH), Yrjö Jahnsson Foundation (Grant No. 6781 to ML), Päivikki and Sakari Sohlberg Foundation (ML), State funding for university-level health research (Hospital District of Helsinki and Uusimaa Grant Nos. TYH2013332, TYH2014228, and TYH2017128 to TK), and European Union's Seventh Framework Programme for project "Integrated neuroimaging and metabolic platform for characterisation of early psychosis and prediction of patient outcomes" (METSY) (Grant No. 602478 to JS).

We thank all the study participants. We also thank Tuula Mononen and Sanna Järvinen for coordinating the data collection and interviews, Marjut Grainger for managing the data, Marita Kattelus for assisting in the imaging, Enrico Glerean for providing us with data collection software for the movie ratings, and Juho Kettunen for calculating the optic flow.

The movie was presented with license from the Finnish rights holder (M&M Viihdepalvelu Oy, Vantaa, Finland).

Part of these data were presented at the fifth biennial Schizophrenia International Research Society Conference, 2016, Florence, Italy, and the second annual Finnish Symposium on Biological Psychiatry, 2016, Helsinki, Finland.

ML has received financial compensation for an interview from Lundbeck. TK has received rewards for lectures from Oy H. Lundbeck Ab/Otsuka Pharma Scandinavia AB and Janssen-Cilag Oy. The other authors report no biomedical financial interests or potential conflicts of interest.

ARTICLE INFORMATION

From the Mental Health Unit (TM, ER, ML, TK, JS), National Institute for Health and Welfare; Department of Psychology and Logopedics (TM, ER), University of Helsinki; Department of Psychiatry (TK, TTR), University of Helsinki, Helsinki University Hospital; Department of Art (RH), School of Arts, Design and Architecture, Aalto University, Helsinki; Department of Neuroscience and Biomedical Engineering (TM, LN, ER, RH, TTR) and Advanced Magnetic Imaging Center (TM, LN, ER, RH, TTR), Aalto NeuroImaging, Aalto University School of Science, Espoo; and Turku PET Centre (LN) and Department of Psychology (LN), University of Turku, Turku, Finland.

Address correspondence to Teemu Mäntylä, M.A., Mental Health Unit, National Institute for Health and Welfare, PO Box 30, Helsinki FI-00271, Finland; E-mail: teemu.mantyla@thl.fi.

Received Nov 15, 2017; revised Apr 16, 2018; accepted Apr 22, 2018.

Supplementary material cited in this article is available online at https://doi.org/10.1016/j.biopsych.2018.04.014.

REFERENCES

1. Friston KJ (1998): The disconnection hypothesis. Schizophr Res 30:115–125.
2. Rubinov M, Bullmore E (2013): Schizophrenia and abnormal brain network hubs. Dialogues Clin Neurosci 15:339–349.
3. Stephan KE, Friston KJ, Frith CD (2009): Dysconnection in schizophrenia: From abnormal synaptic plasticity to failures of self-monitoring. Schizophr Bull 35:509–527.
4. Goghari VM, Sponheim SR, MacDonald AW 3rd (2010): The functional neuroanatomy of symptom dimensions in schizophrenia: A qualitative and quantitative review of a persistent question. Neurosci Biobehav Rev 34:468–486.
5. Crossley NA, Mechelli A, Ginestet C, Rubinov M, Bullmore ET, McGuire P (2016): Altered hub functioning and compensatory activations in the connectome: A meta-analysis of functional neuroimaging studies in schizophrenia. Schizophr Bull 42:434–442.
6. Bertolero MA, Yeo BTT, D'Esposito M (2015): The modular and integrative functional architecture of the human brain. Proc Natl Acad Sci U S A 112:E6798–E6807.
7. Crossley NA, Mechelli A, Vértes PE, Winton-Brown TT, Patel AX, Ginestet CE, *et al.* (2013): Cognitive relevance of the community structure of the human brain functional coactivation network. Proc Natl Acad Sci U S A 110:11583–11588.
8. Hasson U, Honey CJ (2012): Future trends in neuroimaging: Neural processes as expressed within real-life contexts. Neuroimage 62:1272–1278.
9. Binder JR, Desai RH, Graves WW, Conant LL (2009): Where is the semantic system? A critical review and meta-analysis of 120 functional neuroimaging studies. Cereb Cortex 19:2767–2796.
10. Hasson U, Chen J, Honey CJ (2015): Hierarchical process memory: Memory as an integral component of information processing. Trends Cogn Sci 19:304–313.
11. Damoiseaux JS, Rombouts SA, Barkhof F, Scheltens P, Stam CJ, Smith SM, *et al.* (2006): Consistent resting-state networks across healthy subjects. Proc Natl Acad Sci U S A 103:13848–13853.
12. Hasson U, Nir Y, Levy I, Fuhrmann G, Malach R (2004): Intersubject synchronization of cortical activity during natural vision. Science 303:1634–1640.
13. Byrge L, Dubois J, Tyszka JM, Adolphs R, Kennedy DP (2015): Idiosyncratic brain activation patterns are associated with poor social comprehension in autism. J Neurosci 35:5837–5850.
14. Hasson U, Avidan G, Gelbard H, Vallines I, Harel M, Minshew N, *et al.* (2009): Shared and idiosyncratic cortical activation patterns in autism revealed under continuous real-life viewing conditions. Autism Res 2:220–231.
15. Salmi J, Roine U, Glerean E, Lahnakoski J, Nieminen-von Wendt T, Tani P, *et al.* (2013): The brains of high functioning autistic individuals do not synchronize with those of others. Neuroimage Clin 3:489–497.
16. Anderson JS, Nielsen JA, Ferguson MA, Burback MC, Cox ET, Dai L, *et al.* (2013): Abnormal brain synchrony in Down syndrome. Neuroimage Clin 2:703–715.
17. Guo CC, Nguyen VT, Hyett MP, Parker GB, Breakspear MJ (2015): Out-of-sync: Disrupted neural activity in emotional circuitry during film viewing in melancholic depression. Sci Rep 5:11605.
18. Lerner Y, Bleich-Cohen M, Solnik-Knirsh S, Yogev-Seligmann G, Eisenstein T, Madah W, *et al.* (2018): Abnormal neural hierarchy in processing of verbal information in patients with schizophrenia. Neuroimage Clin 17:1047–1060.
19. van den Heuvel MP, Fornito A (2014): Brain networks in schizophrenia. Neuropsychol Rev 24:32–48.
20. Bullmore E, Sporns O (2009): Complex brain networks: Graph theoretical analysis of structural and functional systems. Nat Rev Neurosci 10:186–198.
21. van den Heuvel MP, Sporns O (2013): Network hubs in the human brain. Trends Cogn Sci 17:683–696.
22. Sepulcre J, Sabuncu MR, Yeo TB, Liu H, Johnson KA (2012): Stepwise connectivity of the modal cortex reveals the multimodal organization of the human brain. J Neurosci 32:10649–10661.
23. Zamora-López G, Zhou C, Kurths J (2010): Cortical hubs form a module for multisensory integration on top of the hierarchy of cortical networks. Front Neuroinform 4:1.
24. van den Heuvel MP, Sporns O (2013): An anatomical substrate for integration among functional networks in human cortex. J Neurosci 33:14489–14500.
25. Rikandi E, Pamilo S, Mäntylä T, Suvisaari J, Kieseppä T, Hari R, *et al.* (2017): Precuneus functioning differentiates first-episode psychosis patients during the fantasy movie Alice in Wonderland. Psychol Med 47:495–506.
26. Ventura J, Lukoff D, Nuechterlein KH, Liberman RP, Green MF, Shaner A (1993): Appendix 1: Brief Psychiatric Rating Scale (BPRS) Expanded version (4.0) scales, anchor points and administration manual. Int J Methods Psychiatr Res 3:227–244.
27. First MB, Spitzer RL, Gibbon M, Williams JBW (2007): Structured Clinical Interview for DSM-IV-TR Axis I Disorders, Research Version, Patient Edition (SCID-I/P). New York: Biometrics Research, New York State Psychiatric Institute.
28. Mäntylä T, Mantere O, Raij TT, Kieseppä T, Laitinen H, Leiviskä J, *et al.* (2015): Altered activation of innate immunity associates with white matter volume and diffusion in first-episode psychosis. PLoS One 10:e0125112.
29. Suckling J, Ohlssen D, Andrew C, Johnson G, Williams SCR, Graves M, *et al.* (2008): Components of variance in a multicentre functional MRI study and implications for calculation of statistical power. Hum Brain Mapp 29:1111–1122.
30. Kauppi J, Jääskeläinen IP, Sams M, Tohka J (2010): Inter-subject correlation of brain hemodynamic responses during watching a movie: Localization in space and frequency. Front Neuroinform 4:5.
31. Forsyth JK, McEwen SC, Gee DG, Bearden CE, Addington J, Goodyear B, *et al.* (2014): Reliability of functional magnetic resonance imaging activation during working memory in a multi-site study: Analysis from the North American Prodrome Longitudinal Study. Neuroimage 97:41–52.
32. Gee DG, McEwen SC, Forsyth JK, Haut KM, Bearden CE, Addington J, *et al.* (2015): Reliability of an fMRI paradigm for emotional processing in a multisite longitudinal study. Hum Brain Mapp 36:2558–2579.
33. Raij TT, Mäntylä T, Mantere O, Kieseppä T, Suvisaari J (2016): Cortical salience network activation precedes the development of delusion severity. Psychol Med 46:2741–2748.
34. Tzourio-Mazoyer N, Landeau B, Papathanassiou D, Crivello F, Etard O, Delcroix N, *et al.* (2002): Automated anatomical labeling of activations in SPM using a macroscopic anatomical parcellation of the MNI MRI single-subject brain. Neuroimage 15:273–289.
35. Yeo BTT, Krienen FM, Sepulcre J, Sabuncu MR, Lashkari D, Hollinshead M, *et al.* (2011): The organization of the human cerebral cortex estimated by intrinsic functional connectivity. J Neurophysiol 106:1125–1165.
36. Viinikainen M, Glerean E, Jääskeläinen IP, Kettunen J, Sams M, Nummenmaa L (2012): Nonlinear neural representation of emotional feelings elicited by dynamic naturalistic stimulation. Open J Neurosci 2:4.
37. van Kerkoerle T, Self MW, Roelfsema PR (2017): Layer-specificity in the effects of attention and working memory on activity in primary visual cortex. Nat Commun 8:13804.
38. Petkov CI, Kang X, Alho K, Bertrand O, Yund EW, Woods DL (2004): Attentional modulation of human auditory cortex. Nat Neurosci 7:658–663.

39. Jäncke L, Mirzazade S, Joni Shah N (1999): Attention modulates activity in the primary and the secondary auditory cortex: A functional magnetic resonance imaging study in human subjects. Neurosci Lett 266:125–128.
40. Treue S (2001): Neural correlates of attention in primate visual cortex. Trends Neurosci 24:295–300.
41. Posner MI, Gilbert CD (1999): Attention and primary visual cortex. Proc Natl Acad Sci U S A 96:2585–2587.
42. Poghosyan V, Ioannides AA (2008): Attention modulates earliest responses in the primary auditory and visual cortices. Neuron 58:802–813.
43. Nichols TE, Holmes AP (2002): Nonparametric permutation tests for functional neuroimaging: A primer with examples. Hum Brain Mapp 15:1–25.
44. Jenkinson M, Bannister P, Brady M, Smith S (2002): Improved optimization for the robust and accurate linear registration and motion correction of brain images. Neuroimage 17:825–841.
45. Andreasen NC, Pressler M, Nopoulos P, Miller D, Ho B (2010): Antipsychotic dose equivalents and dose-years: A standardized method for comparing exposure to different drugs. Biol Psychiatry 67:255–262.
46. Haukka J, Suvisaari J, Tuulio-Henriksson A, Lönnqvist J (2007): High concordance between self-reported medication and official prescription database information. Eur J Pharmacol 63:1069–1074.
47. Buckner RL, Sepulcre J, Talukdar T, Krienen FM, Liu H, Hedden T, *et al.* (2009): Cortical hubs revealed by intrinsic functional connectivity: Mapping, assessment of stability, and relation to Alzheimer's disease. J Neurosci 29:1860–1873.
48. Pamilo S, Malinen S, Hotta J, Seppä M (2015): A correlation-based method for extracting subject-specific components and artifacts from group-fMRI data. Eur J Neurosci 42:2726–2741.
49. Yan C, Zang Y (2010): DPARSF: A MATLAB toolbox for pipeline data analysis of resting-state fMRI. Front Syst Neurosci 4:13.
50. Adolphs R, Nummenmaa L, Todorov A, Haxby JV (2016): Data-driven approaches in the investigation of social perception. Philos Trans R Soc Lond B Biol Sci 371:20150367.
51. Hasson U, Malach R, Heeger DJ (2010): Reliability of cortical activity during natural stimulation. Trends Cogn Sci 14:40–48.
52. Ben-Yakov A, Honey CJ, Lerner Y, Hasson U (2012): Loss of reliable temporal structure in event-related averaging of naturalistic stimuli. Neuroimage 63:501–506.
53. Uhlhaas PJ, Singer W (2010): Abnormal neural oscillations and synchrony in schizophrenia. Nat Rev Neurosci 11:100–113.
54. Javitt DC, Freedman R (2015): Sensory processing dysfunction in the personal experience and neuronal machinery of schizophrenia. Am J Psychiatry 172:17–31.
55. Anticevic A, Corlett PR (2012): Cognition-emotion dysinteraction in schizophrenia. Front Psychol 3:392.
56. Zhang R, Wei Q, Kang Z, Zalesky A, Li M, Xu Y, *et al.* (2015): Disrupted brain anatomical connectivity in medication-naïve patients with first-episode schizophrenia. Brain Struct Funct 220:1145–1159.
57. van den Heuvel MP, Mandl RCW, Stam CJ, Kahn RS, Hulshoff Pol HE (2010): Aberrant frontal and temporal complex network structure in schizophrenia: A graph theoretical analysis. J Neurosci 30:15915–15926.
58. Lynall M, Bassett DS, Kerwin R, McKenna PJ, Kitzbichler M, Muller U, *et al.* (2010): Functional connectivity and brain networks in schizophrenia. J Neurosci 30:9477–9487.
59. Cheng H, Newman S, Goñi J, Kent JS, Howell J, Bolbecker A, *et al.* (2015): Nodal centrality of functional network in the differentiation of schizophrenia. Schizophr Res 168:345–352.
60. Collin G, Kahn RS, de Reus MA, Cahn W, van den Heuvel MP (2014): Impaired rich club connectivity in unaffected siblings of schizophrenia patients. Schizophr Bull 40:438–448.
61. Drakesmith M, Caeyenberghs K, Dutt A, Zammit S, Evans CJ, Reichenberg A, *et al.* (2015): Schizophrenia-like topological changes in the structural connectome of individuals with subclinical psychotic experiences. Hum Brain Mapp 36:2629–2643.
62. Buckner RL, Andrews-Hanna JR, Schacter DL (2008): The brain's default network. Ann N Y Acad Sci 1124:1–38.
63. Zhang S, Li CR (2012): Functional connectivity mapping of the human precuneus by resting state fMRI. Neuroimage 59:3548–3562.
64. Raichle ME (2015): The brain's default mode network. Annu Rev Neurosci 38:433–447.
65. Vatansever D, Menon DK, Manktelow AE, Sahakian BJ, Stamatakis EA (2015): Default mode dynamics for global functional integration. J Neurosci 35:15254–15262.
66. Margulies DS, Ghosh SS, Goulas A, Falkiewicz M, Huntenburg JM, Langs G, *et al.* (2016): Situating the default-mode network along a principal gradient of macroscale cortical organization. Proc Natl Acad Sci U S A 113:12574–12579.
67. Hasson U, Yang E, Vallines I, Heeger DJ, Rubin N (2008): A hierarchy of temporal receptive windows in human cortex. J Neurosci 28:2539–2550.
68. Lerner Y, Honey CJ, Silbert LJ, Hasson U (2011): Topographic mapping of a hierarchy of temporal receptive windows using a narrated story. J Neurosci 31:2906–2915.
69. Simony E, Honey CJ, Chen J, Lositsky O, Yeshurun Y, Wiesel A, *et al.* (2016): Dynamic reconfiguration of the default mode network during narrative comprehension. Nat Commun 7:12141.
70. Ames DL, Honey CJ, Chow MA, Todorov A, Hasson U (2015): Contextual alignment of cognitive and neural dynamics. J Cogn Neurosci 27:655–664.
71. Liang X, Zou Q, He Y, Yang Y (2013): Coupling of functional connectivity and regional cerebral blood flow reveals a physiological basis for network hubs of the human brain. Proc Natl Acad Sci U S A 110:1929–1934.
72. Tomasi D, Wang G, Volkow ND (2013): Energetic cost of brain functional connectivity. Proc Natl Acad Sci U S A 110:13642–13647.
73. Leech R, Braga R, Sharp DJ (2012): Echoes of the brain within the posterior cingulate cortex. J Neurosci 32:215–222.
74. American Psychiatric Association (2000): Diagnostic and Statistical Manual of Mental Disorders, 4th (text rev.) ed. Washington, DC: American Psychiatric Press.
75. Hilsenroth MJ, Ackerman SJ, Blagys MD, Baumann BD, Baity MR, Smith SR, *et al.* (2000): Reliability and validity of DSM-IV Axis V. Am J Psychiatry 157:1858–1863.
76. Andreasen NC (1982): Negative symptoms in schizophrenia: definition and reliability. Arch Gen Psychiatry 39:784.